Identification of *Arthrinium marii* as causal agent of olive tree dieback in Apulia (southern Italy)

D. Gerin[1], F. Nigro[1-2], F. Faretra[1-2] and S. Pollastro[1-2]

[1]Department of Soil, Plant and Food Sciences and [2]Selge Network, University of Bari Aldo Moro, Via Giovanni Amendola, 165/A, 70126 Bari, Italy

Corresponding author: francesco.faretra@uniba.it

Abstract

Olive (*Olea europaea* L. var. *sativa*) is one of the most economically important tree crops grown in the Mediterranean basin. *Arthrinium* Kunze *ex* Fr. (teleomorph: *Apiospora* Sacc.) is a widespread fungal genus, and *Arthrinium marii* Larrondo & Calvo is a ubiquitous species, found in algae, soil, plants and agricultural communities. *Arthrinium marii* was isolated from olive trees showing dieback from orchards located in Andria and in Fasano, Brindisi (Apulia, southern Italy) and identified based on morphological features and molecular analysis of four genomic regions (ITS, *TUB2*, *TEF1* and *LSU*). Two-year-old olive plants artificially inoculated with three representative *A. marii* isolates showed complete dieback within 6 months and the fungus was re-isolated satisfying Koch's postulates. This is the first report of *A. marii* causing dieback on olive trees that could represent an important threat for olive cultivation.

Olive (*Olea europaea* L. var. *sativa*) is an economically important tree crop of Mediterranean countries and the European Union is the leading world producer of olive oil and drupes (FAOSTAT, 2017).

Although olive trees are very resistant to environmental stresses, several biotic entities can compromise their health. Fungal species as those belonging to the genus *Verticillium* are well known as vascular pathogens causing tree wilt, while fungi such as *Botryosphaeriaceae* spp. (*Diplodia* spp., *Dothiorella iberica*, *Lasiodiplodia theobromae*, *Neofusicoccum mediterraneum*), *Cytospora oleina*, *Eutypa lata*, *Phoma incompta*, *Phaeomoniella chlamydospora* and *Phaeoacremonium* spp. were found associated to olive tree decline, dieback and cankers and more recently have acquired great importance worldwide (Romero et al., 2005; Tosi and Natalini, 2009; Ivic et al., 2010; Moral et al., 2010; Rhouma et al., 2010; Kaliterna et al., 2012; Carlucci et al., 2013, 2015; Nigro et al., 2013, 2014; Úrbez-Torres et al., 2013).

A new olive cropping system consisting of intensive or super-intensive plantings is expanding worldwide in order to increase productivity and profits (Tous et al., 2010). About 140 trees/ha as plants density in traditional growing system become up to 400 and 2,500 trees/ha respectively, in intensive and super-intensive growing systems (Russo et al., 2018).

These systems are characterized by different microclimatic conditions because they require a more intensive use of irrigation and fertilization, as compared to traditional growing systems, as

well as by application of mechanical pruning and harvesting and, consequently, the trees are more susceptible to diseases and pests (Graniti et al., 2011). In fact, in intensive and super-intensive growing systems *Pseudomonas savastanoi* pv. *savastanoi* increased on branches and twigs, because the major injuries caused by machinery used in the crop management (Tous et al., 2010). Additionally, an increasing in the Verticillium wilt was ascertained (Jiménez-Díaz et al., 2011; López-Escudero and Mercado-Blanco, 2011).

In 2018, dieback of about 30% of the trees was observed in three two-year-old olive orchards of cv. Arbosana located in Andria and Fasano, Brindisi (Apulia, southern Italy) and in this study the causes of the dieback were explored.

Materials and Methods

Sampling and fungal isolation

About 30% of olive trees (cv. Arbosana) showing dieback were observed in three two-year-old orchards located in Andria, and in Fasano, Brindisi (Apulia, southern Italy). Ten representative symptomatic trees per orchard were randomly sampled and analyzed for wood symptoms in comparison with the healthy ones. Discolored wood tissues were surface-disinfested by submerging them for 2 min in 2% sodium hypochlorite solution, washed twice with sterile water, air dried, and then placed onto potato dextrose agar (PDA, infusion from 200 g peeled and sliced potatoes kept at 60°C for 1 h, 20 g dextrose, adjusted to pH 6.5, 20 g agar Oxoid no. 3, per liter) plates. Plates were incubated at 24±1°C in the dark and after five days *Arthrinium* sp. pure cultures were obtained. Three representative monoconidial isolates (DiSSPA_A1; DiSSPA_A2; DiSSPA_A3) were obtained from pure cultures and used for the subsequent analyses.

Morphology and pathogenicity assay

Morphometric characters were assessed on 10-day-old colonies grown on PDA and malt extract agar (MEA; 20 g Malt Extract Oxoid and 20 g agar Oxoid no. 3, per liter) at 25±1°C according to the synoptic keys proposed for *Arthrinium* species identification (Crous and Groenewald, 2013). Three-hundred globose to elongate ellipsoid conidia were measured for each of the three monoconidial isolates DiSSPA_A1-A3, by using an optical microscope DM2500 (Leica Microsystems, Wetzlar, Germany) equipped with an ocular micrometer.

The production of conidia was assessed on 10 days-old MEA and PDA colonies of the three isolates DiSSPA_A1-A3, according to the method described by Crespo-Sempere et al., (2013). For each medium and isolate three replicated plates were used, and data were expressed as number of conidia$\times 10^4/mm^2$ of colony.

The pathogenicity of the DiSSPA_A1-A3 isolates was investigated by artificial inoculation assays of two-year-old olive trees cvs. Arbosana and Cellina di Nardò. Two different inoculation methods based on root- (method 1) and wood-inoculation (method 2) were compared. Briefly, for the method 1, isolates were cultured for 12 days on PDA at 25±1°C in the dark and conidia were scraped from the colony surface, suspended in sterile water added with 0.05% Tween 20, and filtered on Miracloth (Calbiochem, San Diego, California, USA) to remove mycelium fragments. Roots of two-year-old olive trees were opportunely cut at 20 cm in length, fully

immersed in 2.5 liter of a suspension containing 5×10^4 conidia ml^{-1}, and maintained overnight at 25±1°C before planting in 10×10×17 cm plastic pots containing a sand/lime/peat soil mixture. For the method 2, mycelial plugs (4 mm diameter) from the edge of 15-day-old colonies on PDA were placed in artificial wounds (5 mm long and 3 mm deep) under stem bark of olive trees potted as previously described, at 10 cm height from the crown and then protected with a layer of parafilm. Sterile water (method 1) and sterile PDA medium plugs (method 2) were used as the mock inoculated controls and six replicated plants were used for each treatment. Plants were maintained in the greenhouse (25±2°C; 16-h daylight photoperiod) and at 6 months after inoculation (MAI), wood and roots of both the cultivars were inspected for internal symptoms with a destructive assay by dissecting the plants in three portion (about 10-cm each). The re-isolation assay was carried on collecting from each portion five pieces (moving for each about 2 cm from bottom to up) of woody tissue surface disinfested as reported above and placed onto PDA plates. Additionally, at 2, 4 and 6 MAI, the top length (budding) was measured, and canopy symptoms were assessed by using an empirical scale of four classes [0=healthy tree; 1=up to 25% of the tree showed symptoms (foliar chlorosis and necrosis); 2=26-50% of the tree showed symptoms; 3=51-75% of the tree showed symptoms; 4=76-100% of the tree showed symptoms]. Data were used to calculate the McKinney Index (MKI) according to the following formula (McKinney, 1923): $MKI=[\Sigma(f \times v)]/(n \times N) \times 100$, where f is the number of symptomatic trees, v is the value of each class, N is the total number of examined trees, and n the highest value of the classes occurring in the empirical scale.

Data were analyzed by one-way analysis of variance (ANOVA) followed by the Tukey's honestly significant different test (HSD), using CoStat-software (CoHort Software, Monterey, CA, USA), at the significance levels $P \leq 0.05$. In terms of MKI, no differences were observed for inoculated trees among cultivars and isolates by performing a preliminary two-way ANOVA analyses, so all data were used as biological replicates in comparing inoculated- with mock inoculated-trees.

Molecular and phylogenetic analysis

Genomic DNA of the three monoconidial isolates was extracted according to the CTAB-based protocol described by De Miccolis Angelini et al. (2010). Briefly, two-day-old fungal mycelium was collected from sterile cellophane overlapped to PDA plates. Mycelium, powdered under liquid nitrogen, was mixed with 600 µl of CTAB buffer [100 mM Tris-Cl, pH 8.0; 1.4 M NaCl; 20 mM EDTA, pH 8.0; 2% cetyldimethylethylammonium bromide (w/v); 0.2% β-mercaptoethanol (v/v)]. Samples were frozen and thawed three times using liquid nitrogen and a water bath at 75°C, and then incubated at 75°C for 1 h. After chloroform extraction, the clear supernatant was transferred to a new tube and precipitated with isopropanol. After 30 min at -80°C the pellet, collected by centrifugation at 14,000 rpm for 15 min, was washed with cold 70% ethanol, air-dried, dissolved in TE (10 mM Tris-Cl; 1 mM EDTA, pH 8), treated with 0.1 µg μl^{-1} DNAase-free pancreatic RNAase (Sigma, Milan, Italy) for 2 h at 37°C, and finally precipitated by the addition of 0.6 volumes of 5 M ammonium acetate and 2 vol of cold absolute ethanol. The final DNA pellet, washed with 70% ethanol and air-dried, was dissolved in ultrapure water and stored at -80°C until use. DNA was quantified by using NanoDrop 2000 (Thermo Scientific, MA, USA) and stored at -20°C until use.

The ITS1–5.8S–ITS2 rDNA (ITS) region, translation elongation factor 1-α (*TEF1*), β-tubulin (*TUB2*) and large subunit (*LSU*) of rDNA were amplified by using the primers listed in Table 1.

Amplifications were performed in 50 µL of reaction volume containing 1× buffer (Takara Shuzo, Otsu, Japan), 2.5 mM of $MgCl_2$, 100 nM of each dNTP, 100 nM of each primer, 1 U of Taq polymerase and 100 ng of DNA template. PCR program consisted of an initial denaturation (94°C, 3 min), 35 cycles made up by denaturation (94°C, 1 min), annealing (58°C, 30 s) and extension (72°C, 1 min), followed by a final extension (72°C, 7 min).

PCR products were visualized on a 1.5% agarose gel (110 V for 110 min) and custom-sequenced (Genewiz Inc., Takeley, United Kingdom). Sequences were singularly analyzed for high sequence similarity through BLASTn by searching in the entire nucleotide collection database of GenBank (https://www.ncbi.nlm.nih.gov), and also limiting the search to the sequences from type material.

All ITS, *TEF1*, and *TUB2* sequences of *Arthrinium* sp. (GeneBank accession numbers in Table 2) were previously aligned separately by using SeqMan Pro software (DNASTAR Madison, USA; alignment parameters: Match size=5; Minimum match percentage=10; Maximum gaps per kb in sequence=130) and only the sequences of 33 isolates (including 9 type specimens) that showed at least 80% identity with those of the isolates DiSSPA_A1-A3 were trimmed with SeqMan Pro Software in order to obtain the concatenated ITS-*TEF1*-*TUB2* sequences. The *LSU* sequences were excluded because only few *Arthrinium* sp. sequences were available. Phylogenetic analyses were conducted in MEGA v.6 (Tamura et al., 2013) using the maximum parsimony (MP) and maximum likelihood (ML) methods. The MP tree was obtained using the Subtree-Pruning-Regrafting (SPR) algorithm with search level 1, in which the initial trees were obtained by the random addition of sequences (10 replicates). For ML analysis, MEGA used to infer the best model of nucleotide substitution for the dataset using the Tamura-Nei model and the nearest neighbor interchange (NNI) heuristic search method. For both MP and ML, the branch stability was determined by 1000 bootstrap replicates. *Nigrospora zimmermanii* ITS-*TEF1*-*TUB2* concatenated sequence was used as the outgroup.

Results

Symptoms description, fungal isolation and pathogenicity

Symptomatic trees exhibited foliar chlorosis and twig defoliations. Wood discolorations were observed on transversal and longitudinal wood sections of branches and twigs and colonies morphologically referable to *Arthrinium* sp. were predominantly obtained on PDA (Fig. 1).

Olive trees (cvs. Arbosana and Cellina di Nardò) were artificially inoculated with the three *A. marii* isolates DiSSPA_A1-A3. Exclusively on *A. marii*-inoculated trees, no budding was observed up to 6 MAI, when complete dieback occurred. Conversely, non-inoculated control trees grew about 10 cm per month (Fig. 2). At all the times, no statistically significant differences among isolates and cultivar were ascertained (F and *P* always $\leq$1.6 and $\geq$0.2, respectively) by analyses of inoculated trees. On the contrary, inoculated- and mock inoculated-trees differed statistically in both root- and wood- inoculation assays (Table 3). The MKI was 0.0% on non-inoculated control plants, while, it was of 33.3%, 63.9% and 86.1% in the root-inoculated trees and 19.4%, 38.9% and 63.9% in wood-inoculated ones, at 2, 4 and 6 MAI, respectively.

At the end of the experiment (6 MAI), arthrinium-like colonies were always re-isolated from discolored woody tissues, 25 to-30 cm away from the inoculation point (stem or roots) of the inoculated plants, (cvs. Arbosana and Cellina di Nardò). Moreover, around 30% of roots showed discolorations only in roots-inoculated trees with *A. marii*. No arthrinium-like colonies were obtained from non-inoculated control trees. Other fungi morphologically characterized such as *Trichoderma*, *Alternaria* and *Cladosporium* were isolated from all the plants, irrespective of artificial inoculation method.

Morphology of *A. marii* isolates

The morphology of *A. marii* isolates was observed on PDA and MEA after 10 days of incubation at 25°C in the dark. On both media, colonies were flat, spreading with sparse aerial mycelium. In more detail, on PDA the cultures of the three isolates showed an olivaceous-grey surface and olivaceous-grey patches on the reverse surface. On MEA the cultures appeared with white-grey surface and grey patches on the reverse surface (Fig. 4a).

Mycelium consisted of smooth, hyaline, branched and septate hyphae measuring 2 to 4 µm in diameter. Fifteen-days-old PDA cultures exhibited conidiophores in form of conidiogenous cells that were aggregated in clusters on brown (Fig. 4b), smooth, and ampulliform hyphae, producing conidia (Fig. 4c,d). Conidia were brown, smooth, granular, globose to elongate ellipsoid and measuring 6 to 13 µm in diameter. Brown, elongated, sterile cells (average 22×5 µm), typical of some *Arthrinium* species (Samuels et al., 1981) were also observed (Fig. 4e).

Finally, for all isolates, the conidia production was higher on MEA (3.2 to-5.0×10^4 conidia/mm^2) with respect to PDA (5.5 to-8.4×10^4 conidia/mm^2) (Table 4).

Molecular and phylogenetic analysis

Sequences of 567, 833, 262 and 727 were obtained by sequencing the partial ITS, *LSU*, *TEF1* and *TUB2* regions, respectively of the three *A. marii* isolates DiSSPA_A1-A3 (Table 2).

BLASTn analysis against the entire nucleotide collection database of GeneBank revealed that all sequences showed 99 to-100% identity (coverage = 99 to-100%, e-value = 0.0) with different *Arthrinium* species. In more detail, for the three isolates, the ITS region showed 100% similarity with *A. marii*, *Arthrinium* sp. and *A. phaeospermum* (e.g. KF144900.1; MH355544.1; KY081461.1), the *LSU* showed 99% similarity with *A. marii*, *Arthrinium* sp. and *A. arundinis* (e.g. KF144946.1; MH109530.1; KF993394.1), the *TEF1* showed 99% similarity with *A. marii* (e.g. KF145034.1), and the *TUB2* showed 100% similarity with *A. marii* and *A. hispanicum* (KF144992.1 and AB220289.1). Although none of them was a type specimen, *A. marii* was the only species showing the maximum identity for all four analyzed sequences.

Additionally, limiting the BLASTn analysis only against sequences from type material, all sequences (ITS, *LSU*, *TEF1* and *TUB2*) of the three isolates showed 99 to-100% identity (coverage = 99 to-100%, e-value = 0.0) with *A. marii* type specimen (CBS 497.90, accession numbers in Table 2). The ITS and *LSU* regions of the three isolates showed identities over 99%, although less than *A. marii* CBS 497.90, also with *A. guizhouense*, *A. longistromum* and *A. pseudospegazzinii* type specimens (LC5322, MFLU 15-1184 and CBS 102052 strains,

respectively). Finally, identities under 96% with different *Arthrinum* type specimens were observed for *TEF1* and *TUB2* regions.

After the first alignment of ITS, *TUB2* and *TEF1* sequences, 33 out of 56 *Arthrinium* sp. showed identity >80% with the DiSSPA_A1-A3 isolates. The most parsimonious tree obtained by MP analysis of concatenated ITS-*TEF1*-*TUB2* sequences (tree length=545; consistency index=0.608; retention index=0.812; composite index=0.621) is shown in Fig. 3. The analysis using the ML and Tamura-Nei model resulted in a tree was similar to that obtained with MP analysis, and with the highest log likelihood of -7344.64. Both analyses shown that the concatenated ITS-*TEF1*-*TUB2* sequences of all *Arthrinium* isolates obtained with this study clustered with *A. marii* type specimen, albeit with support not more than 91% (Fig. 3).

Discussion

In this study we identified *A. marii* as the causal agent of a severe dieback of olive trees observed in 2018 in three two-year-old olive orchards, cv. Arbosana located in Apulia (southern Italy). The fungus is ubiquitous in nature, and it has been reported in soils, plants and agricultural communities (Agut and Calvo 2004; Oliveira et al., 2012; Crous and Groenewald, 2013; Sharma et al. 2014; Senanayake et al. 2015; Dai et al. 2016; Gnavi et al. 2017; Wang et al. 2018) as well as in green algae (Gnavi et al., 2017). *Arthrinium* Kunze *ex* Fr. is an anamorph genus, which has been traditionally linked to the teleomorph genus *Apiospora* Sacc.

Arthrinium currently comprises 80 species (http://www.indexfungorum.org) and several of them have been documented as plant pathogens and endophytes (Mavragani et al., 2007; Sharma et al., 2014; Wang et al., 2018), although information on fungal biology and disease epidemiology are generally scanty. Reports on *Arthrinium*-diseases are quite recent but different species are known to be pathogens in different host plants, likely due to changes regarding the environmental conditions, cultural practices or the introduction of new cultivars (Mavragani et al., 2007; Crous and Groenewald, 2013; Lo Piccolo et al., 2014). For example, *A. arundinis* causes brown culm streak of *Phyllostachys praecox*, is additionally found on different plant hosts in China (e.g. *Bambusa* sp., *Bothrocaryum controversum*, *Dichotomanthus tristaniaecarpa*, *Phyllostachys* sp. and *Osmanthus* sp.) (Chen et al. 2014; Wang et al. 2018), and it has been also isolated from the leaf of *Hordeum vulgare*, living leaves of *Fagus sylvatica* in Iran and Switzerland and rosemary in Iran (Crous and Groenewald, 2013; Bagherabadi et al., 2014). *Arthrinium sacchari* causes damping-off of durum wheat in the semi-arid Saskatchewan fields (Mavragani et al., 2007). *Arthrinium saccharicola* has been isolated from living and dead culms of *Phragmites australis* and even from the air in the Netherlands and France and from seawater in mangrove habitats in Hong Kong (Crous and Groenewald, 2013; Miao et al. 2006). *Arthrinium xenocordella* is reported as responsible of fruit blight on *Pistacia vera* in Italy (Aiello et al., 2018). *Arthrinium phaeospermum*, responsible of culm rot on *Phyllostachys viridis* (Li et al. 2016), was recently demonstrated to be also associated with necrosis of olive leaves, and according to Koch's postulates the pathogenicity was proved only on leaves and not on twigs (Lo Piccolo et al., 2014). With this study, *A. marii* isolates were collected from branches and twigs of olive trees showing dieback and they reproduced the disease when artificially-inoculated on two-year-old olive plants satisfying Koch's postulates. The fungus was shown to be highly virulent, in fact, at

6 MAI, it was re-isolated 25 to 30 cm away from the inoculation point. A similar behavior was reported for *Botryosphaeria dothidea* and *N. mediterraneum* causing up to 16 cm-lesion on olive branches within 1 MAI (Moral et al., 2010; 2017) and for *Neofabraea kienholzii* and *Phlyctema vagabunda* both isolated from shoot lesions on olive in California and producing lesions up to 4-cm in length at 3 MAI, when inoculated into two-year-old detached shoots (Trouillas et al., 2019).

The morphological features of the three isolates DiSSPA_A1-A3 agreed with those described for *A. marii* by Crous and Groenewald (2013). In addition to the conidia, produced in higher amounts on MEA than on PDA, all isolates (DiSSPA_A1-A3) also produced sterile cells; these features are well known for some *Arthrinium* species, including *A. marii* (Samuels et al., 1981; Crous and Groenewald, 2013).

Examination of morphological features and molecular analysis were both necessary for the appropriate identification of *Arthrinium marii*. Recently, a re-assessment of *Arthrinium* sp. was proposed based on the phylogeny of *LSU* and ITS regions as well as concatenated *TUB2-TEF1* sequences (Crous and Groenewald, 2013). According to the nucleotide BLASTn analysis of ITS, *TUB2*, *TEF1* and *LSU* gene sequences, *A. marii* (type specimen and other isolates) was the only species matching with a high identity (99 to-100%) for all four analyzed sequences. This result was also confirmed by phylogenetic analysis using the concatenated ITS-*TEF1*-*TUB2* sequences. In fact, all isolates (DiSSPA_A1-A3) clustered with the type specimen of *A. marii* (CBS 497.90), although with a support up to 91% of the bootstrap test, and they represented a distinct clade in respect to the other species, including the recently described *A. gaoyouense* (Jiang et al., 2018). Additionally, our results confirm that the strain CBS 114803, identified as *A. marii*, seems to represent an independent lineage as recently reported by Pintos et al. (2019).

In conclusion, to our knowledge this is the first report of *A. marii*, a fungal species that seems ubiquitous in nature, as an agent of severe dieback of olive trees in southern Italy.

The spread of the fungus could represent a serious threat for olive cultivation, also due to the challenges of the new planting systems (intensive and super-intensive) as well due to the introduction into agricultural practice of new varieties more adapted to the new growing system. Generally, the number of fungal species reported as causal agents of trees' decline and dieback is increasing and the interactions established by different fugal species inhabiting olive trees are unknown (Graniti et al., 2011; Nigro et al., 2013, 2014). Additionally, fertilizers and biostimulants obtained from biomasses of different origin, including algae, are available on the market and commonly applied in agriculture because they are considered eco-friendly, but information on the effect of the algae-mycobiota on cultivated plants are scanty. *Arthrinium marii*, for instance, is a component of the mycobiota of the Mediterranean green alga *Flabellia petiolata* (Gnavi et al., 2017), as well as the calcareous brown alga *Padina pavonica* (Garzoli et al., 2018). It is crucial to improve basic knowledge on the microbial community interacting in the complex olive pathosystem in order to implement adequate protection strategies.

Acknowledgements

This research was partially carried out in the framework of the Projects: (i) "Laboratory network for the selection, characterization and conservation of germplasm and for preventing the spread

of economically-relevant and quarantine pests (SELGE) No. 14", funded by the Apulia Region, PO FESR 2007-2013 - Axis I, Line of intervention 1.2., Action 1.2.1; and (ii) Epidemiology, genetics of plant pathogens and development of molecular diagnostic methods granted by the University of Bari.

Author Contributions

Gerin D., Pollastro S., Nigro F. and Faretra F. conceived and planned the experiments, Gerin D. and Nigro F. performed the experiments; Gerin D. and Pollastro S., took the lead in writing the manuscript. Pollastro S., Nigro F. and Faretra F. supervised the research. All authors contributed to the interpretation of the results, provided critical feedback and helped shape the research, analysis and manuscript.

Literature cited

Aiello, D., Gulisano, S., Gusella, G., Polizzi, G., Guarnaccia, V. (2018). First Report of Fruit Blight Caused by *Arthrinium xenocordella* on *Pistacia vera* in Italy. Plant Dis., 102:1853.

Agut, M., Calvo, M. A. (2004). In vitro conidial germination in *Arthrinium aureum* and. *Arthrinium phaeospermum*. Mycopathologia, 157:363-367.

Bagherabadi, S., Zafari, D., Anvar, F.G. (2014). First report of leaf spot caused by *Arthrinium arundinis* on rosemary in Iran. J. Plant Pathol., 96:126.

Carbone, I., Kohn, L.M. (1999). A method for designing primer sets for speciation studies in filamentous *Ascomycetes*. Mycologia, 91:553-556.

Carlucci, A., Raimondo, M.L., Cibelli, F., Phillips, A.J., Lops, F. (2013). *Pleurostomophora richardsiae*, *Neofusicoccum parvum* and *Phaeoacremonium aleophilum* associated with a decline of olives in southern Italy. Phytopathol. Mediterr., 52:517-527.

Carlucci, A., Lops, F., Cibelli, F., Raimondo, M.L. (2015). *Phaeoacremonium* species associated with olive wilt and decline in Southern Italy. Eur. J. Plant Pathol., 141:717-729.

Chen, K., Wu. X.Q., Huang, M.X., Han, Y.Y. (2014). First report of brown culm streak of *Phyllostachys praecox* caused by *Arthrinium arundinis* in Nanjing, China. Plant Dis., 98: 1274.

Crespo-Sempere, A., Marin, S., Sanchis, V., Ramos, A.J. (2013). *VeA* and *LaeA* transcriptional factors regulate ochratoxin A biosynthesis in *Aspergillus carbonarius*. Int. J. Food Microbiol., 166:479-486

Crous, P.W., Groenewald, J.Z. (2013). A phylogenetic re-evaluation of *Arthrinium*. IMA fungus, 4:133-154.

Dai, D. Q., Jiang, H. B., Tang, L. Z., Bhat, D. J. (2016). Two new species of *Arthrinium* (*Apiosporaceae*, *Xylariales*) associated with bamboo from Yunnan, China. Mycosphere, 7:1332-1345.

De Miccolis Angelini, R.M., Habib, W., Rotolo, C., Pollastro, S., Faretra, F. (2010). Selection, characterization and genetic analysis of laboratory mutants of *Botryotinia fuckeliana* (Botrytis cinerea) resistant to the fungicide boscalid. Eur. J. Plant Pathol., 128:185-199.

FAOSTAT (2017). FAO statistical databases. Agriculture data collection (crops).

Garzoli, L., Poli, A., Prigione, V., Gnavi, G., Varese, G. C. (2018). Peacock tail with a fungal cocktail: first assessment of the mycobiota associated with the brown alga *Padina pavonica*. Fungal Ecol., 24:87-97.

Glass, N.L., Donaldson, G.C. (1995). Development of primer sets designed for use with the PCR to amplify conserved genes from filamentous ascomycetes. Appl. Environ. Microb., 61:1323-1330.

Gnavi, G., Garzoli, L., Poli, A., Prigione, V., Burgaud, G-A., Varese, G.C., (2017) The culturable mycobiota of *Flabellia petiolata*: First survey of marine fungi associated to a Mediterranean green alga. PLoS ONE 12:e0175941.

Graniti, A., Faedda, R., Cacciola, S.O., di San Lio, G.M., (2011). Olive diseases in a changing ecosystem. In: L. Schena, G.E. Agosteo, S.O. Cacciola, eds. Olive Diseases and Disorders. Transworld Research Network: Kerala, India, 403-433.

Ivic, D., Ivanovic, A., Milicevic T., Cvjetkovic, B. (2010). Shoot necrosis of olive caused by *Phoma incompta*. Phytopathol.. Mediterr., 49:414-416.

Jiang, N., Li, J., Tian, C.M . (2018). *Arthrinium* species associated with bamboo and reed plants in China. Fungal Syst. and Evol., 2:1-9.

Jiménez-Díaz, R.M., Olivares-García, C., Landa, B. B., del Mar Jiménez-Gasco, M., Navas-Cortés, J. A. (2011). Region-wide analysis of genetic diversity in *Verticillium dahliae* populations infecting olive in southern Spain and agricultural factors influencing the distribution and prevalence of vegetative compatibility groups and pathotypes. Phytopathology, 101:304-315.

Kaliterna, J., Milicevic, T., Ivic, D., Bencic, D., Mesic, A. (2012). First report of *Diplodia seriata* as causal agent of olive dieback in Croatia. Plant Dis., 96:290-290.

Li, B. J., Liu, P. Q., Jiang, Y., Weng, Q. Y., Chen, Q. H. (2016) First report of culm rot caused by *Arthrinium phaeospermum* on *Phyllostachys viridis* in China. Plant Dis., 100:1013.

López-Escudero, F.J., Mercado-Blanco, J. (2011). Verticillium wilt of olive: a case study to implement an integrated strategy to control a soil-borne pathogen. Plant Soil, 344:1-50.

Lo Piccolo, S., Mondello, V., Giambra, S., Conigliaro, G., Torta, L., Burruano, S. (2014). *Arthrinium phaeospermum*, *Phoma cladoniicola* and *Ulocladium consortiale*, new olive pathogens in Italy. J. Phytopathol., 162:258-263.

Mavragani, D.C., Abdellatif, L., McConkey, B., Hamel, C., Vujanovic, V. (2007). First report of damping-off of durum wheat caused by *Arthrinium sacchari* in the semi-arid Saskatchewan fields. Plant Dis., 91:469-469.

McKinney, H. H., (1923). Influence of soil temperature and moisture on infection of wheat seedlings by *Helmintosporium sativum*. J. Agric. Res., 26:195-218.

Miao, L., Kwong, T. F. N., Qian, P. -Y. (2006). Effect of culture conditions on mycelial growth, antibacterial activity, and metabolite profiles of the marine-derived fungus *Arthrinium* c.F. *saccharicola*. Appl. Microbiol. Biotechnol., 72:1063-1073.

Moral, J., Muñoz-Díez, C., González, N., Trapero, A., Michailides, T.J. (2010). Characterization and pathogenicity of *Botryosphaeriaceae* species collected from olive and other hosts in Spain and California. Phytopathology, 100:1340-1351.

Moral, J., Agustí-Brisach, C., Pérez-Rodríguez, M., Xaviér, C., Raya, M.C., Rhouma, A., Trapero, A. (2017). Identification of fungal species associated with branch dieback of olive and resistance of table cultivars to *Neofusicoccum mediterraneum* and *Botryosphaeria dothidea*. Plant disease, 101:306-316.

Nigro, F., Boscia, D., Antelmi, I., Ippolito, A. (2013). Fungal species associated with a severe decline of olive in southern Italy. J.Plant Pathol., 95:668.

Nigro, F., Antelmi, I., Ippolito, A. (2014). Identification and characterization of fungal species associated with the quick decline of olive. International Symposium on the European Outbreak of Xylella fastidiosa in Olive. J. Plant Pathol., 96:101.

O'Donnell, K., Cigelnik, E. (1997). Two divergent intragenomic rDNA ITS2 types within a monophyletic lineage of the fungus *Fusarium* are non-orthologous. Mol. Phylogenet. Evol., 7:103-116.

Oliveira, I., Pereira, J.A., Lino-Neto, T., Bento, A., Baptista, P. (2012). Fungal diversity associated to the olive moth, *Prays oleae* Bernard: a survey for potential entomopathogenic fungi. Microb. Ecol., 63:964-974.

Pintos, Á., Alvarado, P., Planas, J., Jarling, R. (2019). Six new species of *Arthrinium* from Europe and notes about *A. caricicola* and other species found in Carex spp. hosts. MycoKeys, 49:15-48.

Rhouma, A., Triki, M.A., Krid, S., Tuset, J.J., Msallem, M. (2010). First report of a branch dieback of olive trees in Tunisia caused by a *Phoma* sp. Plant Dis., 94:636-636.

Romero, M.A., Sánchez, M.E., Trapero, A. (2005). First report of *Botryosphaeria ribis* as a branch dieback pathogen of olive trees in Spain. Plant Dis., 89:20.

Russo, C., Cappelletti, G., Nicoletti, G., Di Noia, A., & Michalopoulos, G. (2016). Comparison of European olive production systems. Sustainability, 8:825.

Samuels, G.J., McKenzie, E.H.C., Buchanan, D.E. (1981). Ascomycetes of New Zealand 3. Two new species of *Apiospora* and their *Arthrinium* anamorphs on bamboo. New Zeal. J. Bot., 19:137-149.

Senanayake, I.C., Maharachchikumbura, S.S., Hyde, K.D., Bhat, J.D., Jones, E.G., McKenzie, E.H., Dai, D.Q., Daranagama, D.A., Dayarathne, M.C., Goonasekara, I.D., Konta, S., Li, W.J., Qiu, J.S., Stadler M., Wijayawardene, N.N., Xiao, Y.P., Norphanphoun, C., Li, Q., Liu, X.Z., Bahkali, A.H., Kang, J.C., Wang, Y., Wen, T.C., Wendt, L., Xu, J.C., Camporesi, E. (2015). Towards unraveling relationships in *Xylariomycetidae* (*Sordariomycetes*). Fungal Divers., 73:73-144.

Sharma, R., Kulkarni, G., Sonawane, M. S., Shouche, Y.S. (2014). A new endophytic species of *Arthrinium* (*Apiosporaceae*) from *Jatropha podagrica*. Mycoscience, 55:118-123.

Tamura, K., Stecher, G., Peterson, D., Filipski, A., Kumar, S. (2013). MEGA6: molecular evolutionary genetics analysis version 6.0. Mol. Biol. Evol., 30:2725-2729.

Tosi, L., Natalini, G. (2009). First report of *Eutypa lata* causing dieback of olive trees in Italy. Plant Pathol., 58:398-398.

Tous, J., Romero, A., Hermoso, J.F. (2010). New trends in olive orchard design for continuous mechanical harvesting. Adv. Hort. Sci., 24:43-52.

Trouillas, F.P., Nouri, M.T., Lawrence, D.P., Moral, J., Travadon, R., Aegerter, B., Lightle, D. (2019). Identification and characterization of *Neofabraea kienholzii* and *Phlyctema vagabunda* causing leaf and shoot lesions of olive in California. Plant Disease (doi: 391 https://doi.org/10.1094/PDIS-02-19-0277-RE).

Úrbez-Torres, J.R., Peduto, F., Vossen, P.M., Krueger, W.H., Gubler, W. D. (2013). Olive twig and branch dieback: etiology, incidence, and distribution in California. Plant Dis., 97:231-244.

Vilgalys, R., Sun, B.L. (1994). Ancient and recent patterns of geographic speciation in the oyster mushroom *Pleurotus* revealed by phylogenetic analysis of ribosomal DNA sequences. Proc. Natl Acad. Sci. USA, 91:4599-4603.

Wang, M., Tan, X-M., Liu, F., Cai, L. (2018) Eight new *Arthrinium* species from China. MycoKeys, 34:1-24.

White, T.J., Bruns, T., Lee, S.J.W.T., Taylor, J.L. (1990). Amplification and direct sequencing of fungal ribosomal RNA genes for phylogenetics. PCR protocols: a guide to methods and applications, 18:315-322.

Captions

Figure 1. Apical shoots of healthy (a) and symptomatic (b) two-years-old olive plants along with wood discoloration from which the 7-day-old *Arthrinium marii* colonies were obtained on PDA.

Figure 2. Olive plants inoculated or not with *Arthrinium marii*. (a) Detail of budding in *A. marii* inoculated and non-inoculated plants at 2 Months After Inoculation (MAI); (b) general status of leaves at 2, 4 and 6 MAI of *A. marii* inoculated and non-inoculated trees. Arrows indicate the absence of budding in the inoculated tree and bracket marks budding of non-inoculated tree.

Figure 3. Phylogenetic tree of concatenated *ITS-TEF1-TUB2* sequences of *Arthrinium* spp. generated by both maximum parsimony (MP) and maximum likelyhood (ML) methods analysis. In the figure the percentage of replicate trees in which the associated taxa clustered together in the bootstrap test (1000 replicates) are shown on the nodes (MP/ML). *Nigrospora zimmermanii* was used as the outgroup. *: Type specimens.

Figure 4. Morphology of the *Arthrinium marii* DiSSPA_A1 isolated from olive trees: (a) up and bottom side of PDA and MEA cultures; (b) details of PDA colony after 10 and 15 days; (c) conidia and conidiogenous cell; (d) conidia; and (e) sterile cells. In c, d and e bars represent 10 μm and observations refer to a 15 days-old PDA cultures.

Table 1. Primers used.

Target gene/region	Primer name	Primer sequence (5'-3')	References
ITS1–5.8S rDNA–ITS2 (ITS) region	ITS5	GGAAGTAAAAGTCGTAACAAGG	White et al., 1990
	ITS4	TCCTCCGCTTATTGATATGC	
Translation elongation factor 1-a (*TEF1-a*)	EF1-728F	CATCGAGAAGTTCGAGAAGG	Carbone and Kohn, 1999
	EF1-986R	TACTTGAAGGAACCCTTACC	
β-tubulin (*TUB2*)	T1	AACATGCGTGAGATTGTAAGT	O'Donnell and Cigelnik, 1997; Glass and Donaldson, 1995
	Bt2b	ACCCTCAGTGTAGTGACCCTTGGC	
Large subunit (LSU) rDNA region	LROR	ACCCGCTGAACTTAAGC	Vilgalys and Sun, 1994
	LR5	TCCTGAGGGAAACTTCG	

Table 2. Details of *Arthrinium* spp. strains used in the BLASTn and phylogenetic analysis.

Species	Strain*	Host	Country	GeneBank accession numbers**		
				ITS	*TUB2*	*TEF1*
A. arundinis	CBS 464.83	*Phragmites australis*	Netherlands	KF144888.1	KF144979.1	KF145021.1
A. arundinis	LC7277	*Bambusa* sp.	China	KY494750.1	KY705218.1	KY705146.1
A. arundinis	EGG3	*Lasioptera donacis*	France	MF627422.1	MF627424.1	MF627423.1
A. bambusae	**LC7106**	*Bambusa* sp.	China	KY494719.1	KY705187.1	KY705117.1
A. bambusae	LC7113	*Bambusa* sp.	China	KY494720.1	KY705188.1	KY806205.1
A. bambusae	LC7124	*Bambusa* sp.	China	KY494727.1	KY705195.1	KY806206.1
A. camelliae-sinensis	LC8181	*Brassica rapa* subsp. *oleifera*	China	KY494761.1	KY705229.1	KY705157.1
A. camelliae-sinensis	**LC5007**	Camellia sinensis	China	KY494704.1	KY705173.1	KY705103.1
A. dichotomanthi	LC8175	*Dichotomanthes tristaniicarpa*	China	KY494755.1	KY705223.1	KY705151.1
A. dichotomanthi	LC8176	*Dichotomanthes tristaniicarpa*	China	KY494756.1	KY705224.1	KY705152.1
A. dichotomanthi	**LC4950**	*Dichotomanthes tristaniicarpa*	China	KY494697.1	KY705167.1	KY705096.1
A. gaoyouense	CFCC52301	*Phragmites australis*	China	MH197124	MH236789.1	MH236793.1
A. gaoyouense	CFCC52302	*Phragmites australis*	China	MH197125	MH236790.1	MH236794.1
A. guizhouense	**LC5322**	Air	China	KY494709.1	KY705178.1	KY705108.1
A. guizhouense	LC5318	Air	China	KY494708.1	KY705177.1	KY705107.1
A. jiangxiense	LC2831	*Bambusa* sp.	China	KY494686.1	KY806201.1	KY705085.1
A. jiangxiense	**LC4577**	*Maesa* sp.	China	KY494693.1	KY705163.1	KY705092.1
A. jiangxiense	LC5394	Soil	China	KY494711.1	KY705180.1	KY705110.1
A. kogelbergense	CBS 117206	Unknown algae	Croatia	KF144895.1	KF144987.1	KF145029.1
A. kogelbergense	**CBS 113333**	*Restionaceae*	South Africa	KF144893.1	KF144985.1	KF145027.1
A. kogelbergense	CBS 114734	*Uncus gerardii*	Sweden	KF144894.1	KF144986.1	KF145028.1
A. hydei	LC7103	*Bambusa* sp.	China	KY494715.1	KY705183.1	KY705114.1
A. hydei	**CBS 114990**	*Bambusa tuldoides*	China	KF144890.1	KF144982.1	KF145024.1
A. malaysianum	**CBS 102053**	*Macaranga hullettii*	Malaysia	KF144896.1	KF144988.1	KF145030.1
A. malaysianum	CBS 251.29	*Cinnamomum camphora*	Unknown	KF144897.1	KF144989.1	KF145031.1
A. marii	CPC 18904	*Phragmites australis*	Italy	KF144902.1	KF144994.1	KF145036.1
A. marii	**CBS 497.90**	-	Spain	MH862232.1	KF144993.1	KF145035.1
A. marii	CBS 200.57	*Beta vulgaris*	Netherlands	KF144900.1	KF144992.1	KF145034.1
A. marii	CBS 114803	*Pseudosasa hindsii*	China	KF144899.1	KF144991.1	KF145033.1
*A. marii****	DiSSPA_A1	*Olea europaea*	Italy	MK602320.1	MK614695.1	MK645472.1
*A. marii****	DiSSPA_A1	*Olea europaea*	Italy	MK602321.1	MK614696.1	MK645473.1
*A. marii****	DiSSPA_A1	*Olea europaea*	Italy	MK602322.1	MK614697.1	MK645474.1
A. obovatum	LC8177	*Lithocarpus* sp.	China	KY494757.1	KY705225.1	KY705153.1
A. obovatum	LC8178	*Lithocarpus* sp.	China	KY494758.1	KY705226.1	KY705154.1
A. obovatum	**LC4940**	*Lithocarpus* sp.	China	KY494696.1	KY705166.1	KY705095.1
A. ovatum	CBS 115042	*Arundinaria hindsii*	China	KF144903.1	KF144995.1	KF145037.1
A. phaeospermum	CBS 142.55	Soil	Japan	KF144908.1	KF145000.1	KF145042.1
A. phaeospermum	CBS 114318	*Hordeum vulgare*	Itan	KF144907.1	KF144999.1	KF145041.1
A. phaeospermum	CBS 114317	*Hordeum vulgare*	Itan	KF144906.1	KF144998.1	KF145040.1
A. phragmites	CPC:18900	*Phragmites australis*	Italy	KF144909.1	KF145001.1	KF145043.1
A. pseudoparenchymaticum	LC8173	*Bambusa* sp.	China	KY494753.1	KY705221.1	KY705149.1
A. pseudoparenchymaticum	LC8174	*Bambusa* sp.	China	KY494754.1	KY705222.1	KY705150.1
A. pseudoparenchymaticum	**LC7234**	*Bambusa* sp.	China	KY494743.1	KY705211.1	KY705139.1
A. pseudospegazzinii	**CBS 102052**	*Macaranga hullettii*	Malaysia	KF144911.1	KF145002.1	KF145045.1
A. pterospermum	**CPC:20193**	*Lepidosperma gladiatum*	Australia	KF144913.1	KF145004.1	KF145046.1
A. rasikravindrae	LC5449	Unknown	China	KY494713.1	KY705182.1	KY705112.1
A. rasikravindrae	LC7115	*Bambusa* sp.	China	KY494721.1	KY705189.1	KY705118.1
A. rasikravindrae	LC7117	*Bambusa* sp.	China	KY494722.1	KY705190.1	KY705119.1
A. sacchari	CBS 372.67	Air	Unknown	KF144918.1	KF145007.1	KF145049.1
A. sacchari	CBS 664.74	Soil	Netherlands	KF144919.1	KF145008.1	KF145050.1
A. sacchari	CBS 301.49	*Bambusa* sp.	Indonesia	KF144917.1	KF145006.1	KF145048.1
A. saccharicola	CBS 831.71	Unknown	Netherlands	KF144922.1	KF145012.1	KF145054.1
A. saccharicola	CBS 463.83	*Phragmites australis*	Netherlands	KF144921.1	KF145011.1	KF145053.1
A. saccharicola	CBS 191.73	Unknown	Netherlands	KF144920.1	KF145009.1	KF145051.1
A. subroseum	LC7215	*Bambusa* sp.	China	KY494740.1	KY705208.1	KY705136.1
A. subroseum	LC7291	*Bambusa* sp.	China	KY494751.1	KY705219.1	KY705147.1
A. thailandicum	LC5630	Unknown	China	KY494714.1	KY806200.1	KY705113.1
A. xenocordella	**CBS 478.86**	Soil	Zimbabwe	KF145013.1	KF144925.1	KF145055.1
A. xenocordella	LC3486	*Camellia sinensis*	China	KY494687.1	KY705158.1	KY705086.1

*CBS: Westerdijk Fungal Biodiversity Institute, Utrecht, The Netherlands; CPC: Culture collection of Pedro Crous, housed at Westerdijk Fungal Biodiversity Institute; LC: working collection of Lei Cai, housed at Institute of Microbiology, Chinese Academy of Sciences, Beijing, China. **ITS: partial ITS1–5.8S rDNA–ITS2; *Tub2*: β-tubulin; *Tef1*: translation elongation factor 1-alpha. ***for the isolates DiSSPA_A1, DiSSPA_A2 and DiSSPA_A3 the accession numbers of the rDNA large subunit regions (LSU) sequences, used in the BLASTn analysis were MK604516, MK604517 and MK604518, respectively. Bold: type specimens.

Table 3. McKinney's Index for olive trees artificially inoculated with *Arthrinium marii*.

Inoculation with	2 MAI	4 MAI	6 MAI
wood-inoculation			
A. marii	19.4±2.8 a	38.9±4.8 a	63.9±2.8 a
Control	0.0±0.0 b	0.0±0.0 b	0.0±0.0 b
root-inoculation			
A. marii	33.3±0.0 a	63.9±2.8 a	86.1±2.8 a
Control	0.0±0.0 b	0.0±0.0 b	0.0±0.0 b

Data represent the mean values ± standard error. MAI: months after inoculation. For each MAI and inoculation assay, data followed by different letters were statistically significant at probability levels $P \leq 0.05$ according to the Tukey's test.

Table 4. Conidia production by *Arthrinium marii* isolates.

Isolate	Conidia (No. x 10^4/mm^2)	
	PDA	MEA
DiSSPA_A1	3.2±0.4	6.6±0.9
DiSSPA_A2	5.0±0.7	8.4±0.6
DiSSPA_A3	3.2±0.5	5.5±0.7

Data represent the mean values ± standard error.

Table 1. Primers used.

Target gene/region	Primer name	Primer sequence (5'-3')	References
ITS1–5.8S rDNA–ITS2 (ITS) region	ITS5	GGAAGTAAAAGTCGTAACAAGG	White et al., 1990
	ITS4	TCCTCCGCTTATTGATATGC	
Translation elongation factor 1-a (*TEF1-a*)	EF1-728F	CATCGAGAAGTTCGAGAAGG	Carbone and Kohn, 1999
	EF1-986R	TACTTGAAGGAACCCTTACC	
β-tubulin (*TUB2*)	T1	AACATGCGTGAGATTGTAAGT	O'Donnell and Cigelnik, 1997; Glass and Donaldson, 1995
	Bt2b	ACCCTCAGTGTAGTGACCCTTGGC	
Large subunit (LSU) rDNA region	LROR	ACCCGCTGAACTTAAGC	Vilgalys and Sun, 1994
	LR5	TCCTGAGGGAAACTTCG	

Table 2. Details of *Arthrinium* spp. strains used in the BLASTn and phylogenetic analysis.

Species	Strain*	Host	Country	GeneBank accession numbers**		
				ITS	*TUB2*	*TEF1*
A. arundinis	CBS 464.83	*Phragmites australis*	Netherlands	KF144888.1	KF144979.1	KF145021.1
A. arundinis	LC7277	*Bambusa* sp.	China	KY494750.1	KY705218.1	KY705146.1
A. arundinis	EGG3	*Lasioptera donacis*	France	MF627422.1	MF627424.1	MF627423.1
A. bambusae	**LC7106**	*Bambusa* sp.	China	KY494719.1	KY705187.1	KY705117.1
A. bambusae	LC7113	*Bambusa* sp.	China	KY494720.1	KY705188.1	KY806205.1
A. bambusae	LC7124	*Bambusa* sp.	China	KY494727.1	KY705195.1	KY806206.1
A. camelliae-sinensis	LC8181	*Brassica rapa* subsp. *oleifera*	China	KY494761.1	KY705229.1	KY705157.1
A. camelliae-sinensis	**LC5007**	Camellia sinensis	China	KY494704.1	KY705173.1	KY705103.1
A. dichotomanthi	LC8175	*Dichotomanthes tristaniicarpa*	China	KY494755.1	KY705223.1	KY705151.1
A. dichotomanthi	LC8176	*Dichotomanthes tristaniicarpa*	China	KY494756.1	KY705224.1	KY705152.1
A. dichotomanthi	**LC4950**	*Dichotomanthes tristaniicarpa*	China	KY494697.1	KY705167.1	KY705096.1
A. gaoyouense	CFCC52301	*Phragmites australis*	China	MH197124	MH236789.1	MH236793.1
A. gaoyouense	CFCC52302	*Phragmites australis*	China	MH197125	MH236790.1	MH236794.1
A. guizhouense	**LC5322**	Air	China	KY494709.1	KY705178.1	KY705108.1
A. guizhouense	LC5318	Air	China	KY494708.1	KY705177.1	KY705107.1
A. jiangxiense	LC2831	*Bambusa* sp.	China	KY494686.1	KY806201.1	KY705085.1
A. jiangxiense	**LC4577**	*Maesa* sp.	China	KY494693.1	KY705163.1	KY705092.1
A. jiangxiense	LC5394	Soil	China	KY494711.1	KY705180.1	KY705110.1
A. kogelbergense	CBS 117206	Unknown algae	Croatia	KF144895.1	KF144987.1	KF145029.1
A. kogelbergense	**CBS 113333**	*Restionaceae*	South Africa	KF144893.1	KF144985.1	KF145027.1
A. kogelbergense	CBS 114734	*Uncus gerardii*	Sweden	KF144894.1	KF144986.1	KF145028.1
A. hydei	LC7103	*Bambusa* sp.	China	KY494715.1	KY705183.1	KY705114.1
A. hydei	**CBS 114990**	*Bambusa tuldoides*	China	KF144890.1	KF144982.1	KF145024.1
A. malaysianum	**CBS 102053**	*Macaranga hullettii*	Malaysia	KF144896.1	KF144988.1	KF145030.1
A. malaysianum	CBS 251.29	*Cinnamomum camphora*	Unknown	KF144897.1	KF144989.1	KF145031.1
A. marii	CPC 18904	*Phragmites australis*	Italy	KF144902.1	KF144994.1	KF145036.1
A. marii	**CBS 497.90**	-	Spain	MH862232.1	KF144993.1	KF145035.1
A. marii	CBS 200.57	*Beta vulgaris*	Netherlands	KF144900.1	KF144992.1	KF145034.1
A. marii	CBS 114803	*Pseudosasa hindsii*	China	KF144899.1	KF144991.1	KF145033.1
*A. marii****	DiSSPA_A1	*Olea europaea*	Italy	MK602320.1	MK614695.1	MK645472.1
*A. marii****	DiSSPA_A1	*Olea europaea*	Italy	MK602321.1	MK614696.1	MK645473.1
*A. marii****	DiSSPA_A1	*Olea europaea*	Italy	MK602322.1	MK614697.1	MK645474.1
A. obovatum	LC8177	*Lithocarpus* sp.	China	KY494757.1	KY705225.1	KY705153.1
A. obovatum	LC8178	*Lithocarpus* sp.	China	KY494758.1	KY705226.1	KY705154.1
A. obovatum	**LC4940**	*Lithocarpus* sp.	China	KY494696.1	KY705166.1	KY705095.1
A. ovatum	CBS 115042	*Arundinaria hindsii*	China	KF144903.1	KF144995.1	KF145037.1
A. phaeospermum	CBS 142.55	Soil	Japan	KF144908.1	KF145000.1	KF145042.1
A. phaeospermum	CBS 114318	*Hordeum vulgare*	Itan	KF144907.1	KF144999.1	KF145041.1
A. phaeospermum	CBS 114317	*Hordeum vulgare*	Itan	KF144906.1	KF144998.1	KF145040.1
A. phragmites	CPC:18900	*Phragmites australis*	Italy	KF144909.1	KF145001.1	KF145043.1
A. pseudoparenchymaticum	LC8173	*Bambusa* sp.	China	KY494753.1	KY705221.1	KY705149.1
A. pseudoparenchymaticum	LC8174	*Bambusa* sp.	China	KY494754.1	KY705222.1	KY705150.1
A. pseudoparenchymaticum	**LC7234**	*Bambusa* sp.	China	KY494743.1	KY705211.1	KY705139.1
A. pseudospegazzinii	**CBS 102052**	*Macaranga hullettii*	Malaysia	KF144911.1	KF145002.1	KF145045.1
A. pterospermum	**CPC:20193**	*Lepidosperma gladiatum*	Australia	KF144913.1	KF145004.1	KF145046.1
A. rasikravindrae	LC5449	Unknown	China	KY494713.1	KY705182.1	KY705112.1
A. rasikravindrae	LC7115	*Bambusa* sp.	China	KY494721.1	KY705189.1	KY705118.1
A. rasikravindrae	LC7117	*Bambusa* sp.	China	KY494722.1	KY705190.1	KY705119.1
A. sacchari	CBS 372.67	Air	Unknown	KF144918.1	KF145007.1	KF145049.1
A. sacchari	CBS 664.74	Soil	Netherlands	KF144919.1	KF145008.1	KF145050.1
A. sacchari	CBS 301.49	*Bambusa* sp.	Indonesia	KF144917.1	KF145006.1	KF145048.1
A. saccharicola	CBS 831.71	Unknown	Netherlands	KF144922.1	KF145012.1	KF145054.1
A. saccharicola	CBS 463.83	*Phragmites australis*	Netherlands	KF144921.1	KF145011.1	KF145053.1
A. saccharicola	CBS 191.73	Unknown	Netherlands	KF144920.1	KF145009.1	KF145051.1
A. subroseum	LC7215	*Bambusa* sp.	China	KY494740.1	KY705208.1	KY705136.1
A. subroseum	LC7291	*Bambusa* sp.	China	KY494751.1	KY705219.1	KY705147.1
A. thailandicum	LC5630	Unknown	China	KY494714.1	KY806200.1	KY705113.1
A. xenocordella	**CBS 478.86**	Soil	Zimbabwe	KF145013.1	KF144925.1	KF145055.1
A. xenocordella	LC3486	*Camellia sinensis*	China	KY494687.1	KY705158.1	KY705086.1

*CBS: Westerdijk Fungal Biodiversity Institute, Utrecht, The Netherlands; CPC: Culture collection of Pedro Crous, housed at Westerdijk Fungal Biodiversity Institute; LC: working collection of Lei Cai, housed at Institute of Microbiology, Chinese Academy of Sciences, Beijing, China. **ITS: partial ITS1–5.8S rDNA–ITS2; *Tub2*: β-tubulin; *Tef1*: translation elongation factor 1-alpha. ***for the isolates DiSSPA_A1, DiSSPA_A2 and DiSSPA_A3 the accession numbers of the rDNA large subunit regions (LSU) sequences, used in the BLASTn analysis were MK604516, MK604517 and MK604518, respectively. Bold: type specimens.

Table 3. McKinney's Index for olive trees artificially inoculated with *Arthrinium marii*.

Inoculation assay	2 MAI	4 MAI	6 MAI
wood-inoculation			
A. marii	19.4±2.8 a	38.9±4.8 a	63.9±2.8 a
Control	0.0±0.0 b	0.0±0.0 b	0.0±0.0 b
root-inoculation			
A. marii	33.3±0.0 a	63.9±2.8 a	86.1±2.8 a
Control	0.0±0.0 b	0.0±0.0 b	0.0±0.0 b

Data represent the mean values ± standard error. MAI = months after inoculation. For each MAI and inoculation assay, data followed by different letters were statistically significant at probability level $P \leq 0.05$ according to the Tukey's test.

Table 4. Conidia production by *Arthrinium marii* isolates.

Isolate	Conidia (No. x 10^4/mm^2)	
	PDA	MEA
DiSSPA_A1	3.2±0.4	6.6±0.9
DiSSPA_A2	5.0±0.7	8.4±0.6
DiSSPA_A3	3.2±0.5	5.5±0.7

Data represent the mean values ± standard error.

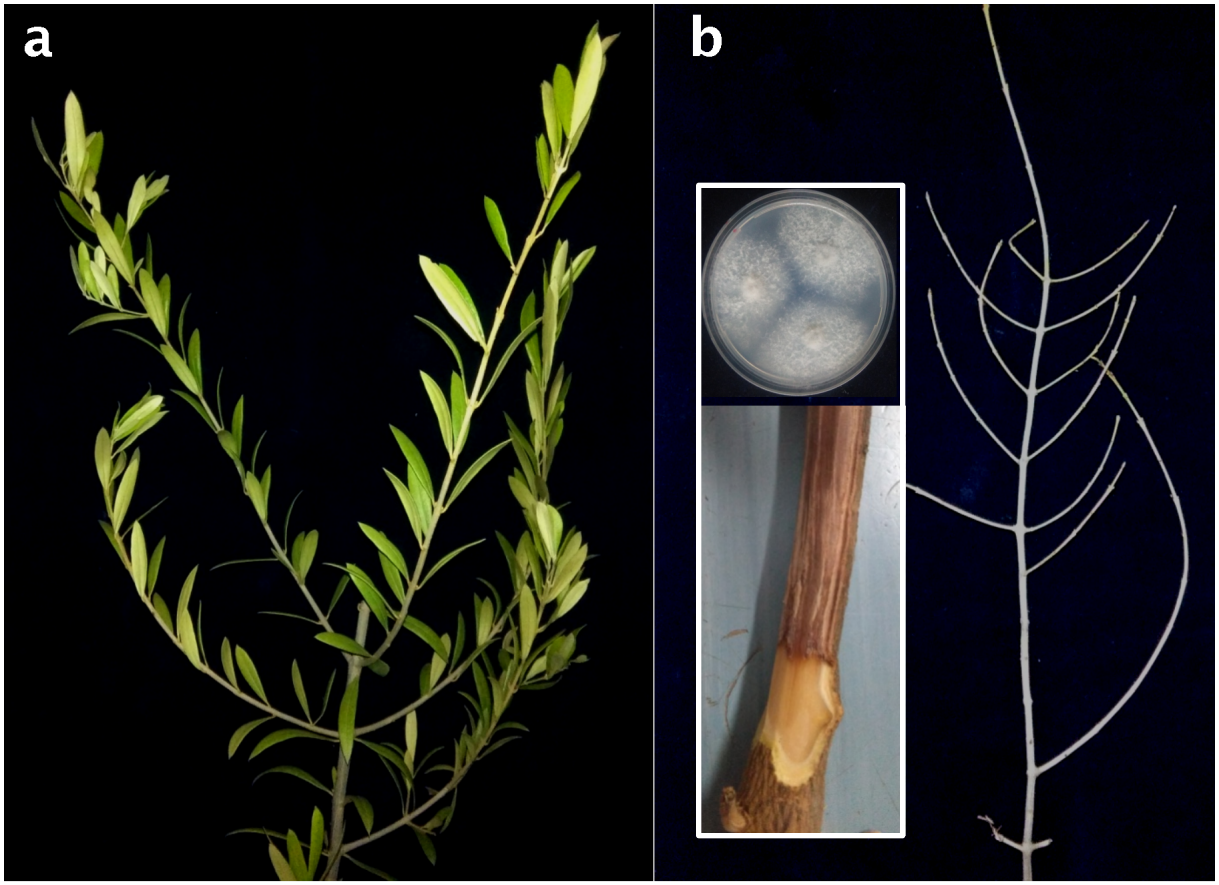
a
b

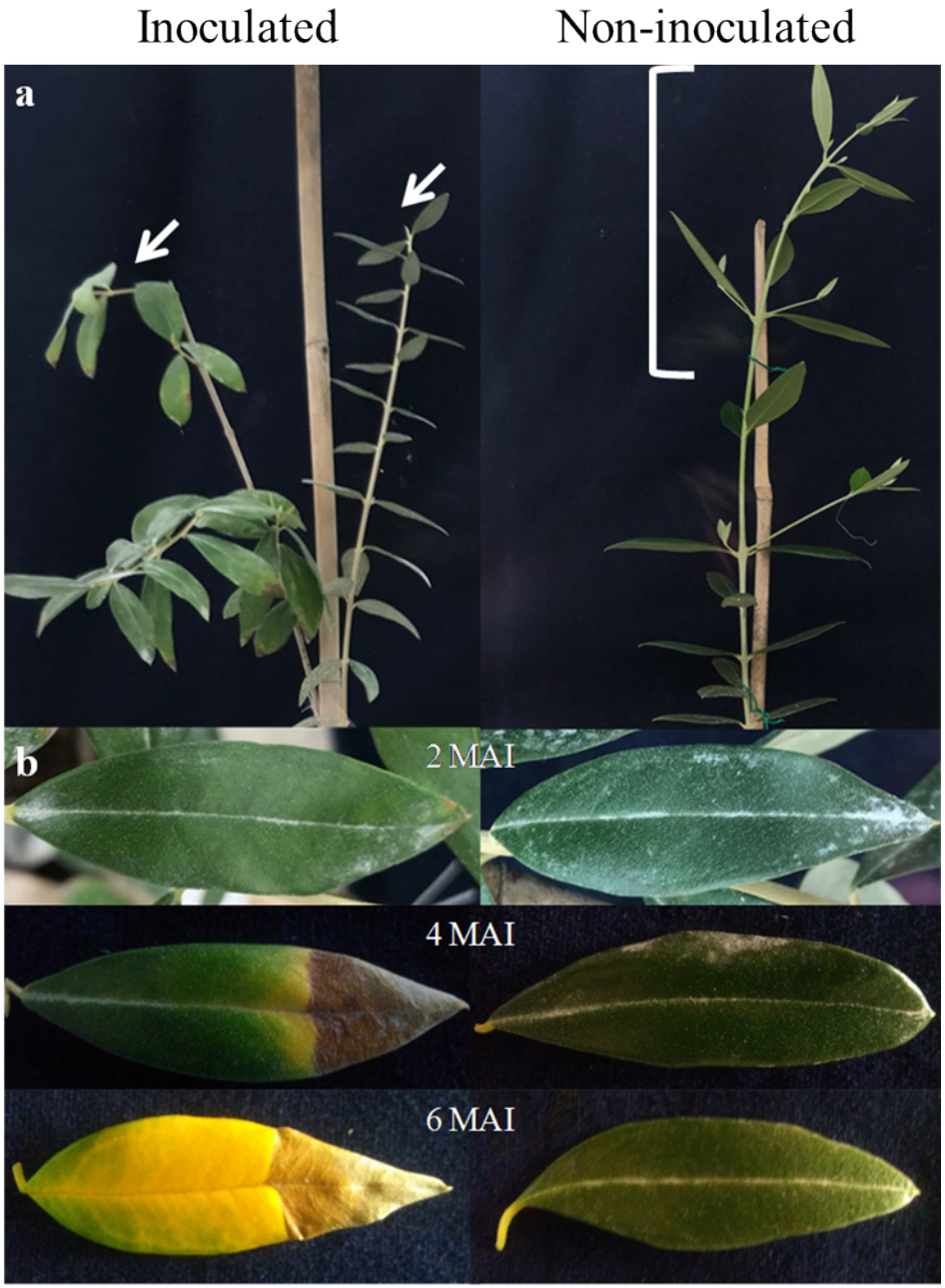
Inoculated
Non-inoculated
a
b
2 MAI
4 MAI
6 MAI

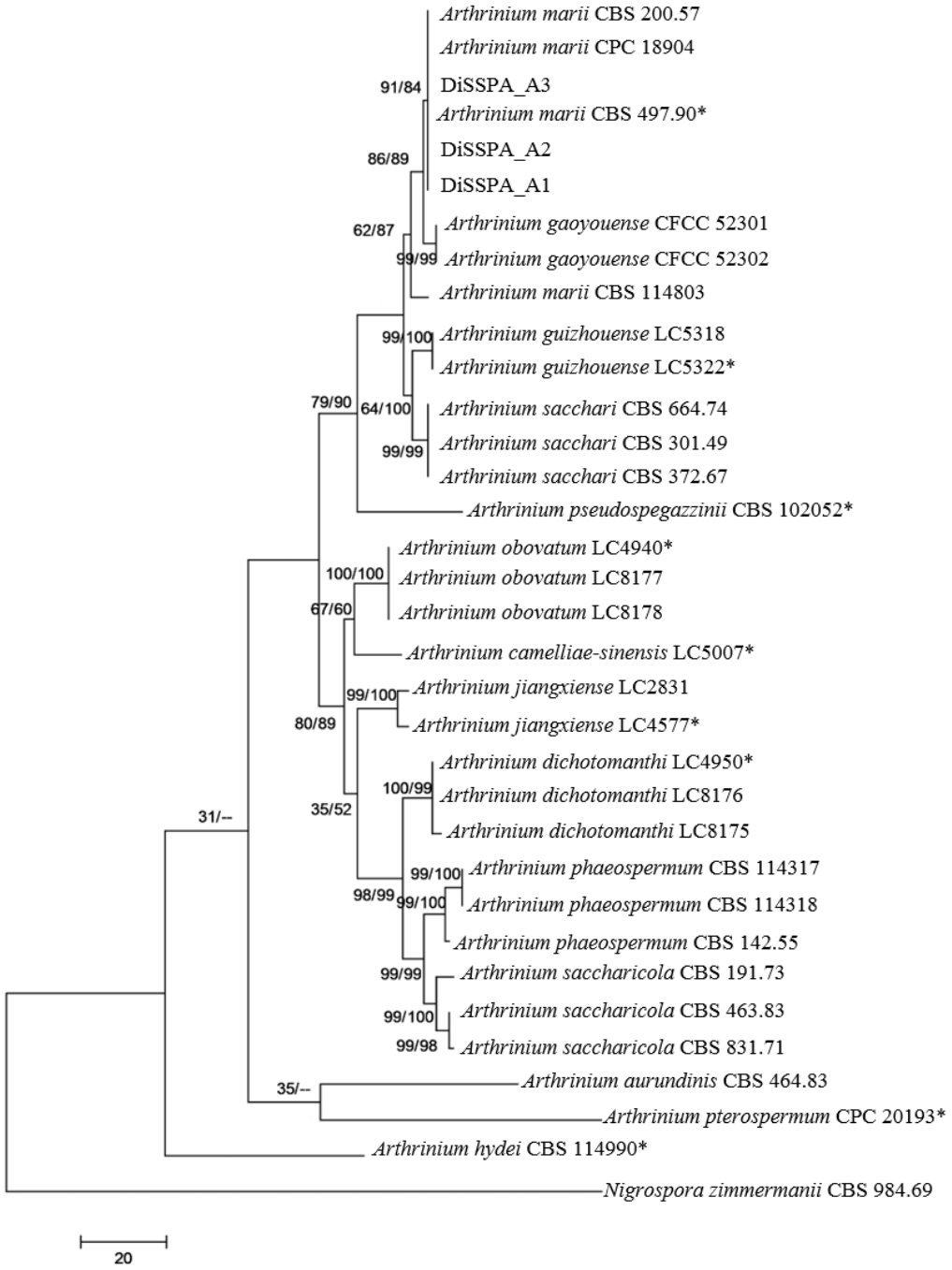
Arthrinium marii CBS 200.57
Arthrinium marii CPC 18904
91/84
DiSSPA_A3
Arthrinium marii CBS 497.90*
86/89
DiSSPA_A2
DiSSPA_A1
62/87
Arthrinium gaoyouense CFCC 52301
99/99
Arthrinium gaoyouense CFCC 52302
Arthrinium marii CBS 114803
99/100
Arthrinium guizhouense LC5318
Arthrinium guizhouense LC5322*
79/90
64/100
Arthrinium sacchari CBS 664.74
99/99
Arthrinium sacchari CBS 301.49
Arthrinium sacchari CBS 372.67
Arthrinium pseudospegazzinii CBS 102052*
Arthrinium obovatum LC4940*
100/100
Arthrinium obovatum LC8177
67/60
Arthrinium obovatum LC8178
Arthrinium camelliae-sinensis LC5007*
99/100
Arthrinium jiangxiense LC2831
80/89
Arthrinium jiangxiense LC4577*
Arthrinium dichotomanthi LC4950*
100/99
Arthrinium dichotomanthi LC8176
35/52
31/--
Arthrinium dichotomanthi LC8175
99/100
Arthrinium phaeospermum CBS 114317
98/99
99/100
Arthrinium phaeospermum CBS 114318
Arthrinium phaeospermum CBS 142.55
99/99
Arthrinium saccharicola CBS 191.73
99/100
Arthrinium saccharicola CBS 463.83
99/98
Arthrinium saccharicola CBS 831.71
35/--
Arthrinium aurundinis CBS 464.83
Arthrinium pterospermum CPC 20193*
Arthrinium hydei CBS 114990*
Nigrospora zimmermanii CBS 984.69
20